Nutritional channels in breast cancer

Alejandro Godoy [a, b], Katherine Salazar [a], Carlos Figueroa [c], Gary J. Smith [b], Maria de los Angeles Garcia [a], Francisco J. Nualart [a, *]

[a] *Departamento de Biología Celular, Universidad de Concepción, Concepción, Chile*
[b] *Department of Urologic Oncology, Roswell Park Cancer Institute, Buffalo, NY, USA*
[c] *Instituto de Histología y Patología, Universidad Austral de Chile, Valdivia, Chile*

Received: July 13, 2008; Accepted: October 7, 2008

Abstract

Breast cancers increase glucose uptake by increasing expression of the facilitative glucose transporters (GLUTs), mainly GLUT1. However, little is known about the relationship between GLUT1 expression and malignant potential in breast cancer. In this study, expression and subcellular localization of GLUT1 was analysed *in vivo* in breast cancer tissue specimens with differing malignant potential, based on the Scarff-Bloom-Richardson (SBRI, II, III) histological grading system, and *in vitro* in the breast cancer cell lines, MDA-MB-468 and MCF-7, and in MDA-MB-468 cells grown as xenografts in nude athymic BALB/c male mice. *In situ* hybridization analyses demonstrated similar levels of GLUT1 mRNA expression in tissue sections from breast cancers of all histological grades. However, GLUT1 protein was expressed at higher levels in grade SBRII cancer, compared with SBRI and SBRIII, and associated with the expression of the proliferation marker PCNA. Immunolocalization analyses in SBRII cancers demonstrated a preferential localization of GLUT1 to the portions of the cellular membrane that faced neighbouring cells and formed 'canaliculi-like structures', that we hypothesize could have a potential role as 'nutritional channels'. A similar pattern of GLUT1 localization was observed in confluent cultures of MDA-MB-468 and MCF-7, and in MDA-MB-468 cells grown as xenografts, but not in the normal breast epithelial cell line HMEC. However, no relationship between GLUT1 expression and malignant potential of human breast cancer was observed. Preferential subcellular localization of GLUT1 could represent a physiological adaptation of a subset of breast cancer cells that form infiltrative tumours with a nodular growth pattern and that therefore need a major diffusion of glucose from blood vessels.

Keywords: glucose • glucose transporter • GLUT1 • breast cancer

Introduction

Breast cancer is the leading cause of cancer death in women in the United States; it is estimated that approximately 180,000 new cases will be diagnosed during 2008 [1]. Breast cancer cells, as most cancer cells, have a high level of glucose uptake and metabolism compared with normal cells [2–4]. Increased glucose uptake by cancer cells is mediated through increased expression of facilitative glucose transporters (GLUTs) [2, 3, 5, 6]. Fourteen members of the mammalian facilitative GLUT family have been identified: GLUT1–12, GLUT14, and the H+/myo-inositol transporter (HMIT). GLUT1 was believed to be the isoform of the facilitative GLUTs expressed ubiquitously in normal tissues, and overexpressed in human cancers [6–8]. However, an analysis of 154 human neoplasms failed to detect GLUT1 in 87 cancers [9]. A study of 118 breast cancers observed expression of GLUT1 in only 42% of the samples [10]. The lack of GLUT1 expression in a significant fraction of cancers suggested that cancers may express other GLUT isoforms [7, 11]. To address this hypothesis, we evaluated 215 different cancers for expression of GLUT1–6 and GLUT9 and confirmed GLUT1 as the most widely expressed isoform in human cancers, with 58% of the samples showing moderate to high levels of immunostaining for GLUT1 [5]. This cellular property has been utilized extensively in positron emission tomography (PET) for noninvasive detection and evaluation of therapeutic response in a wide variety of cancers using the glucose analogue 2-[18F]-fluoro-2-deoxy-D-glucose (FDG) as a radiotracer [12–15]. In addition to expression of GLUT1, human cancers also expressed the GLUT isoforms GLUT2 (31%) and GLUT5 (27%) [5], which

*Correspondence to: Dr. Francisco J. NUALART,
Departamento de Biología Celular,
Facultad de Ciencias Biológicas, Universidad de Concepción,
Casilla 160-C, Concepción, Chile.
Tel.: 56-41-2203479
Fax: 56-41-2245975
E-mail: frnualart@udec.cl

doi:10.1111/j.1582-4934.2008.00544.x

are both fructose transporters. This evidence, along with the established capability of some cancer cell lines to incorporate radiolabelled fructose [5], suggested that, in addition to glucose, fructose may have an important role in maintaining cancer cell metabolism and that fructose uptake also could be used for PET imaging [5, 16].

Even though expression of the facilitative GLUTs in breast cancer have been studied in some detail [5, 10, 17, 18], little is known about the biological contribution of GLUT1 to malignant potential in breast cancer. High level of expression of GLUT1 was correlated with increased aggressiveness and poor prognosis in lung cancer [19–21] and liver vascular tumours [22]. Moreover, GLUT1 overexpression correlated with lymph node metastases and poor prognosis in colorectal cancer [23, 24], and malignant progression in Barrett's oesophagus [25].

Although breast cancers overexpress GLUT1, considerable variability in the level of expression of GLUT1 was observed between different samples [5]. This characteristic could be associated with the histological grade of the tumour, which is usually correlated with the infiltrative and growth pattern, and presence of metastasis. In this study, a detailed characterization of the subcellular localization of GLUT1 in human breast cancer *in vivo* and *in vitro*, and the relationship between GLUT1 expression and malignant potential, based on the Scarff-Bloom-Richardson (SBRI, II, III) histological grading system, was assessed using conventional and ultrastructural immunocytochemistry.

Material and methods

Cell lines and tissue specimens

MCF-7 and MDA-MB-468 cell lines (obtained from American Type Culture Collection ATCC) were cultured in Dulbecco's Modified Eagle's Medium (DMEM) or L-15 medium, respectively. Culture medias were supplemented with 10% foetal calf serum, 100 U/ml of penicillin and 100 μg/ml of streptomycin. Cells were incubated at 37°C in a 5% CO_2 humidified atmosphere. Tissue sections were obtained from 12 different clinical specimens of benign breast and from 36 different specimens of breast cancer with different histological grades based upon the Scarff-Bloom-Richardson system (8 samples of SBRI, 17 samples of SBRII, and 11 samples of SBRIII). The Anatomical Pathology Services at the Valdivia's Hospital and the University of Concepcion of Chile kindly donated the clinical specimens.

Animal studies

Four- to six-week-old nude athymic BALB/c male mice were injected subcutaneously on the flank with the breast cancer cell line MDA-MB-468 at a concentration of 1.0×10^7 cells/ml. Three to four weeks after inoculation, when individual tumours reached approximately 1.0 cm^3, tumours were resected and processed for histologic analysis. All animal experimentation was conducted in accordance with accepted standards of the Ethics Committee at the University of Concepción.

In situ hybridization

A cDNA of approximately 2.5 kb that encoded the human GLUT1 was subcloned into a pcDNA3 vector. RNA probes were transcribed *in vitro* and labelled using digoxigenin-UTP to generate sense and antisense digoxigenin-labelled ribo-probes [26]. Probe size was reduced to approximately 300 nucleotides by alkaline hydrolysis and *in situ* hybridization performed on histological sections of breast cancer tissue. Sections were baked at 60°C for 1 hr, deparaffinized in xylene, and rehydrated in a graded series of ethanol washes. Tissue sections were treated for 5 min. at 37°C with proteinase K (1 μg/ml in PBS, Sigma-Aldrich, St. Louis, MO, USA), fixed with 4% paraformaldehyde for 5 min. at 4°C, washed in cold PBS and acetylated in 0.1 M triethanol amine-HCl (pH 8.0) for 10 min. at room temperature. For *in situ* hybridization, sections were incubated for 15 min. at 37°C in pre-hybridization solution, washed, and incubated in 25 μl of hybridization mix (50% formamide, 0.6 M NaCl, 10 mM Tris-HCl (pH 7.5), 1 mM EDTA, 1× Denhart's solution, 10% PEG 8000, 10 mM DTT, 500 μg yeast tRNA/ml, 50 μg/ml heparin, 500 μg/ml DNA carrier, and riboprobe diluted between 1:20 and 1:100) in a humidified chamber at 42°C overnight. After removal of the coverslips, slides were rinsed twice in 4× SSC for 30 min. at 42°C and washed for 30 min. at 37°C each in 2× SSC, 0.3× SSC, and 0.1× SSC. Digoxigenin was visualized by incubating tissue specimens for 2 hrs with a monoclonal anti-digoxigenin antibody conjugated to alkaline phosphatase. Nitroblue tetrazolium chloride and 5-bromo-4-chloro-3-indolyl-phosphate were used as substrates for alkaline phosphatase.

Immunohistochemistry

Tissue sections were obtained from clinical specimens of benign breast and breast cancers. For immunocytochemical analyses, the normal mammary epithelial cell line (HMEC) and the mammary tumour cell lines (MDA-468 and MCF-7), obtained from ATCC, were fixed *in situ* with 4% (w/v) paraformaldehyde for 30 min. at room temperature. Before incubation with the immunoreagent, endogenous peroxidase activity was inhibited with 0.3% (v/v) H_2O_2 in methanol and non-specific binding of antibody was blocked with 3% (w/v) bovine serum albumin (BSA, EMD Chemicals, Gibbstown, NJ, USA) for 30 min. at room temperature. Histological sections and fixed cells were immunostained using standard methodology [5, 27–29]. Specimens were incubated overnight with affinity purified rabbit polyclonal anti-GLUT1 (1:1000, Alpha Diagnostic, San Antonio, TX, USA) or mouse monoclonal anti-PCNA (DakoCytomation, Carpinteria, CA, USA) primary antibodies diluted in 100 mM Tris-HCl buffer (pH 7.8) that contained 8.4 mM sodium phosphate, 3.5 mM potassium phosphate, 120 mM NaCl, and 1% (w/v) BSA. After washing 3 times in Tris-HCl buffer (pH 7.8) for 10 min. each, specimens were incubated with HRP-conjugated anti-rabbit IgG or anti-mouse IgG (1:100, DakoCytomation) secondary antibody for 2 hrs at room temperature. Peroxidase activity was developed using 3,3-diaminobenzidine tetrahydrochloride (1 μg/ml, Sigma-Aldrich) and H_2O_2 (1 μl/ml, VWR International, West Chester, PA, USA) in 100 mM Tris-HCl buffer (pH 7.8). Haematoxylin was used as a nuclear counterstain in tissue sections. Stained slides were dehydrated through a series of graded alcohol washes to xylene, and mounted with coverslips. For immunofluorescence studies, tissue sections were incubated 2 hrs at room temperature with Cy2- or Cy3-conjugated affinity-purified donkey anti-rabbit or anti-mouse IgG secondary antibody (1:200, Jackson ImmunoResearch Laboratories, West Grove, PA, USA). Topro-3 iodide (Molecular Probes, Carlsbad, CA, USA) was used to visualize nuclei. Immunocytochemistry in the absence of primary antibody, or using preimmune serum, provided negative controls.

Ultrastructural immunocytochemistry

Tissue sections obtained from clinical specimens of breast cancers of the histological grade SBRII were immersed for 1 hr in fixative containing 2% paraformaldehyde and 0.5% glutaraldehyde in 0.1 M phosphate buffer (pH 7.4) [5]. Each sample was redissected, immersed in fresh fixative for 11 hrs, washed for 1 hr with phosphate buffer and postfixed for 1 hr with 0.5% OsO_4 in phosphate buffer. Tissue sections were washed in distilled water for 15 min., dehydrated and embedded in butyl-methyl-methacrylate. Ultrathin sections were mounted on nickel grids, treated with 1% H_2O_2 for 1, 3 or 5 min., washed in distilled water, and rinsed in Tris-HCl buffer (pH 7.8). For immunodetection, the anti-GLUT1 antibody (1:100, Alpha Diagnostic) was diluted in 100 mM Tris-HCl buffer (pH 7.8) that contained 8.4 mM sodium phosphate, 3.5 mM potassium phosphate, 120 mM NaCl and 1% (w/v) BSA and the grids were incubated overnight. After washing, the ultrathin sections were incubated for 2 hrs in a solution containing gold-labelled anti-rabbit IgG (1:20), washed, and incubated with uranyl-acetate/lead citrate to provide contrast. Samples were analysed using a Hitachi H-700 electron microscope with 125–200 kV accelerating voltage. Incubation with pre-immune IgG, or omitting primary antibody, provided negative controls.

TUNEL procedure

Cell death in tissue sections from tumours formed by MDA-MB-468 cells grown as xenografts in nude athymic BALB/c male mice was analysed using the ApopTag TUNEL kit (ONCOR, Gaithersburg, MD, USA) according to the manufacturer's instructions. Briefly, tissue sections were incubated for 5 min. at 37°C with proteinase K (1 μg/ml in PBS, Sigma-Aldrich). After that, tissue sections were incubated for 1 hr at 37°C in working-strength terminal deoxynucleotidyl transferase (TdT) enzyme and dUTP-digoxigenin. Tissue sections were then incubated for 30 min. at room temperature in 100 mM Tris-HCl buffer (pH 7.8) containing fluorescein-conjugated anti-digoxigenin antibody (1:50, Boehringer Ingelheim, Ingelheim, Germany). Immunostaining was visualized using fluorescence microscopy. Negative control sections were treated similarly but incubated in the absence of TdT enzyme, dUTP-digoxigenin or anti-digoxigenin antibody.

Results

GLUT1 expression in human breast cancer tissues with differing malignant potential

The level of expression of GLUT1 in benign breast tissue and breast cancer tissue specimens with differing malignant potential was assessed using *in situ* hybridization and immunohistochemistry (Fig. 1). In benign breast tissue, low-to-undetectable levels of GLUT1 protein expression were observed in benign epithelial glands (G) using immunohistochemistry (Fig. 1A and B, arrows). *In situ* hybridization analysis confirmed this result (data not shown). Low levels of GLUT1 protein expression were detected in the stromal cell compartment (St) of normal breast tissue using immunohistochemistry (Fig. 1A). The majority of the reaction was detected in erythrocytes (E), which confirmed antibody specificity (Fig. 1B). Moreover, low levels of PCNA expression were observed in benign breast tissue (Fig. 1C). In breast cancer tissues, GLUT1 mRNA staining localized to the cytoplasm of the breast cancer cells (CC), and was observed at similar levels of intensity among all histological grades (Fig. 1D, G, J). GLUT1 mRNA was increased in tissue sections from breast cancers of all histological grades (SBRI, SBRII, and SBRIII) compared with benign breast tissue (data not shown). Immunohistochemical studies showed the highest level of GLUT1 protein expression was detected in tumours of histological grade SBRII (Fig. 1H, arrows). In these cancers, GLUT1 immunostaining localized mostly to the plasma membrane in the breast cancer cells (Fig. 1H, arrows and Fig. 2). Cancers of histological grade SBRI and III had lower levels of GLUT1 immunostaining compared with cancers of grade SBRII, even though the levels of GLUT1 mRNA in these samples were comparable to the levels of GLUT1 mRNA observed in tumours of histological grade SBRII. Specifically, tumours of histological grade SBRIII showed a weak and diffuse GLUT1 immunoreaction that was localized predominantly in the cytoplasm of the breast cancer cells (Fig. 1K). Histological grade SBRIII cancers grew in close relationship to the surrounding stroma. Even though highly infiltrative, they do not show a nodular growth pattern, which could explain the low levels of GLUT1 expression. Taken together, these data indicated that the highest levels of expression of GLUT1 protein in breast cancer was observed in tumours of histological grade SBRII. However, the level of protein expression showed no correspondence with GLUT1 mRNA expression or malignant potential.

Expression of GLUT1 and of the proliferation marker PCNA was analysed using immunohistochemistry in benign breast tissue and breast cancer tissue samples with differing malignant potential (Fig. 1). Benign breast tissue samples showed low levels of proliferation demonstrated by low-to-undetectable levels of expression of PCNA (Fig. 1C). In breast cancer tissue specimens, the highest level of proliferation was observed in cancers of histological grade SBRII and SBRIII. Cancers of grade SBRI had the lowest level of expression of PCNA. In all samples, immunoreaction for PCNA showed a specific pattern of nuclear localization (Fig. 1C, F, I, L). Thus, elevated levels of expression of the proliferation marker PCNA in cancers of histological grade SBRII associated with high level of expression of GLUT1.

The relationship between GLUT1 expression and proliferation status was explored at the cellular level in cancers of histological grade SBRII by evaluating GLUT1 and PCNA co-localization using confocal laser scanning microscopy (Fig. 2). Although overexpression of GLUT1 was associated with increased expression of PCNA in cancers of histological grade SBRII at the tissue level, the relationship between GLUT1 and PCNA was variable at the cellular level; although some cancer cells that overexpressed GLUT1 showed expression of PCNA (Fig. 2D–F, arrows and inset), others did not (Fig. 2A–C, inset). However, all cells that showed expression of the proliferation marker PCNA also showed increased expression of GLUT1 in SBRII cancers (Fig. 2D–F and inset).

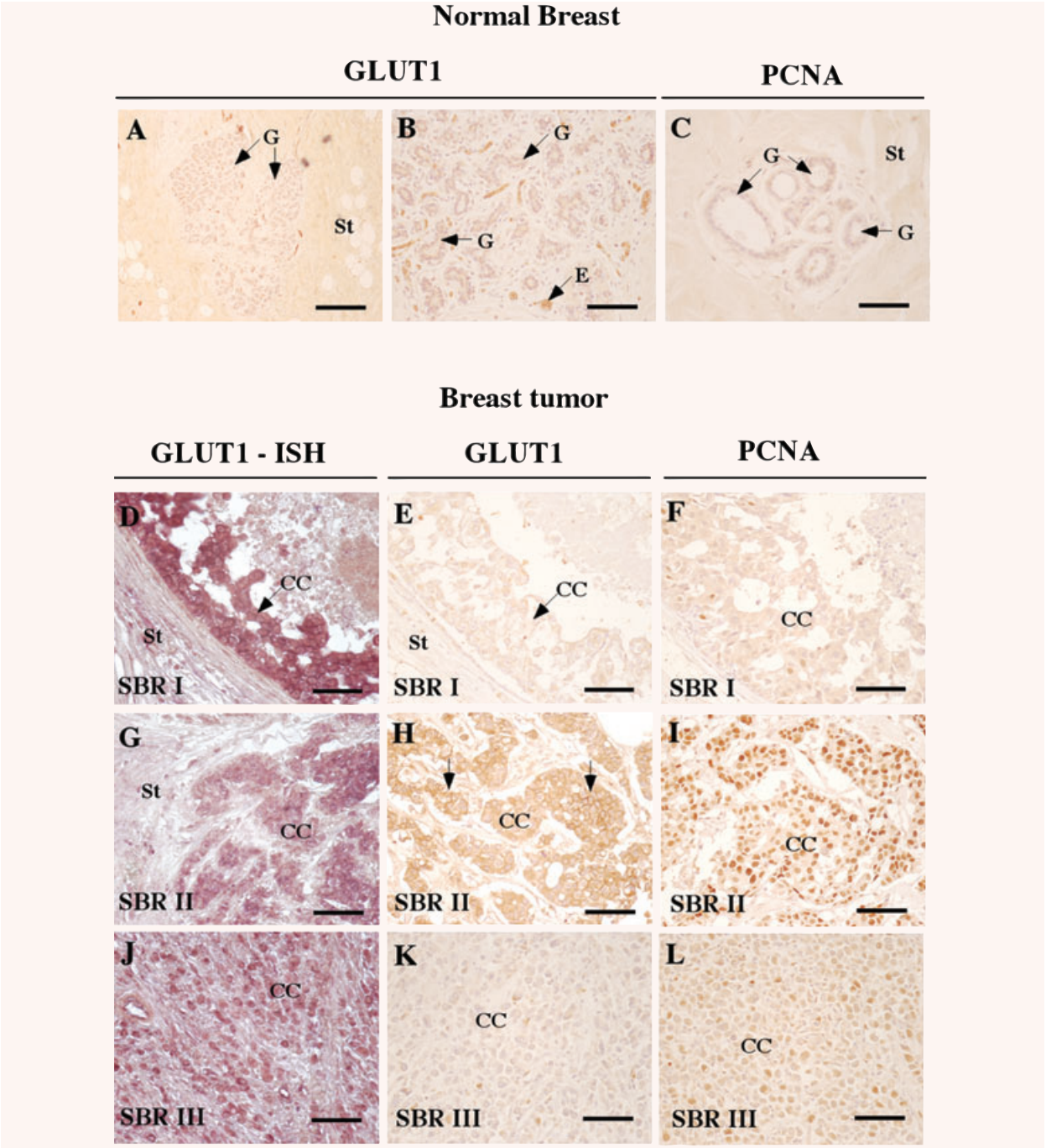

Fig 1. GLUT1 and PCNA expression in benign breast and breast cancer tissue specimens. (**A**, **B**) GLUT1 protein expression in benign breast tissue was analysed using immunohistochemistry. (**C**) PCNA protein expression in benign breast tissue was analysed using immunohistochemistry. (**D**, **E**) GLUT1 mRNA and protein expression analysed using *in situ* hybridization (ISH) and immunohistochemistry, respectively, in grade SBRI breast cancer. (**F**) PCNA protein expression analysed using immunohistochemistry in grade SBRI breast cancer. (**G**, **H**) GLUT1 mRNA and protein expression analysed using ISH and immunohistochemistry, respectively, in grade SBRII breast cancer. (**I**) PCNA protein expression analysed using immunohistochemistry in grade SBRII breast cancer. (**J**, **K**) GLUT1 mRNA and protein expression analysed using ISH and immunohistochemistry, respectively, in grade SBRIII breast cancer. (**L**) PCNA protein expression analysed using immunohistochemistry in grade SBRIII breast cancer. CC, cancer cells; E, blood vessel with erythrocytes; St, stroma; G, glandular tissue. Images **A** ×50, **B–C**: ×80, images **D–L**: ×100.

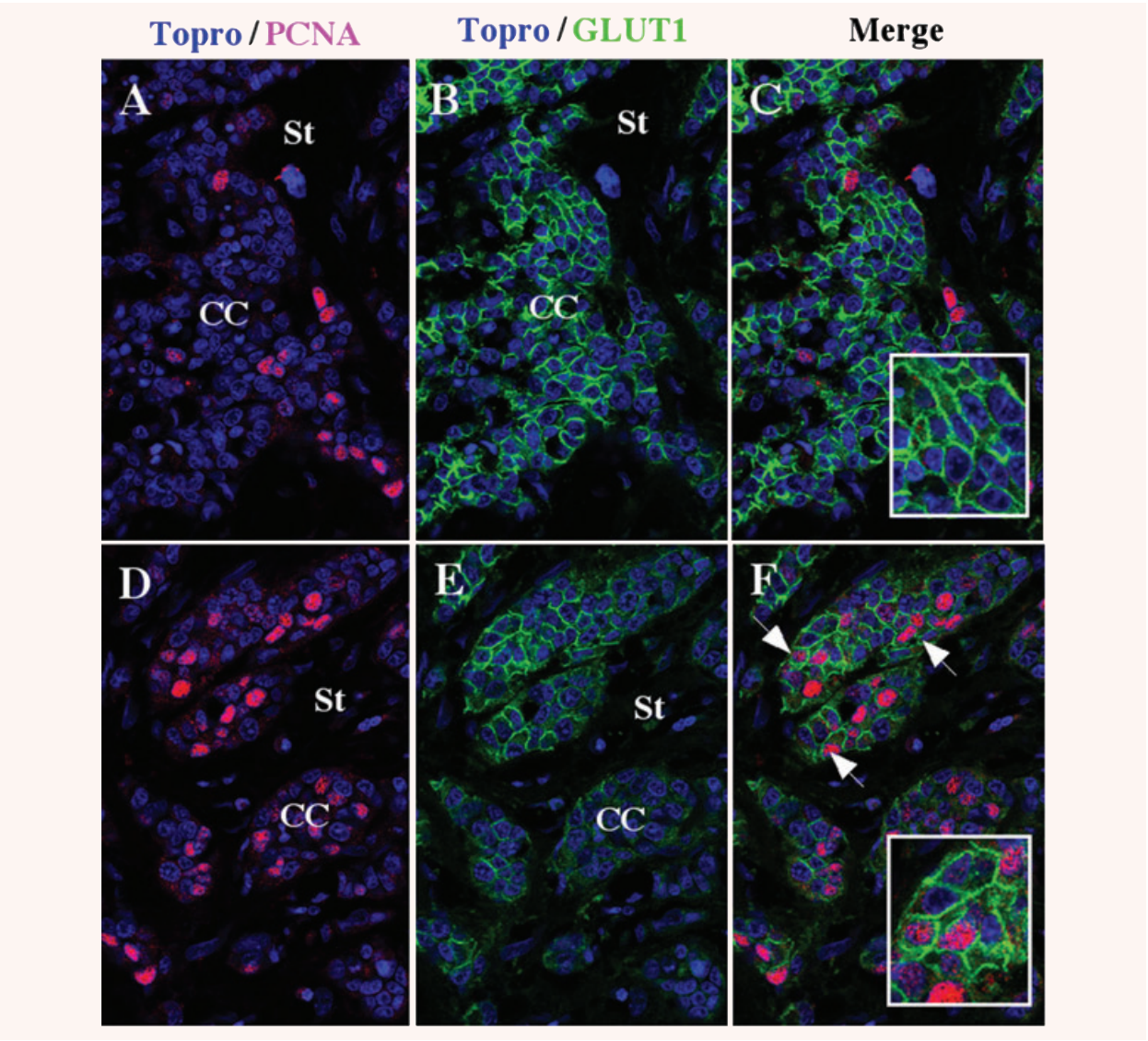

Fig. 2 Colocalization of GLUT1 and PCNA in grade SBRII breast cancer. GLUT1 and PCNA co-localization studies were performed using confocal laser scanning microscopy. GLUT1 and PCNA were immunodetected using Cy2- or Cy3-conjugated affinity-purified donkey anti-rabbit or anti-mouse IgG secondary antibody, respectively. Topro-3 was used to visualize nuclei. Co-expression of GLUT1 and PCNA at the cellular level was variable. A population of cancer cells expressed only GLUT1 (**A**–**C**), whereas another population co-expressed GLUT1 and PCNA (**D**–**F**). CC, cancer cells; St, stroma. Images A–F: ×200. Insets: ×400.

Preferential subcellular localization of GLUT1 to the portion of cellular membranes that form canaliculi-like structures in cancers of histological grade SBRII

Subcellular localization of GLUT1 was analysed using standard immunocytochemistry, immunofluorescence and ultrastructural immunocytochemistry in tissue sections of breast cancers of histological grade SBRII (Figs. 3 and 4). The level of intensity of the GLUT1 immunostaining was elevated in breast cancer cells compared with the surrounding stroma (Fig. 3A). GLUT1 showed a heterogeneous level of expression within cancer parenchymal cells. Higher levels of GLUT1 immunoreaction were observed at the centre of the tumour mass, where cellular density was increased (Fig. 3A–E). At the cellular level, GLUT1 localized

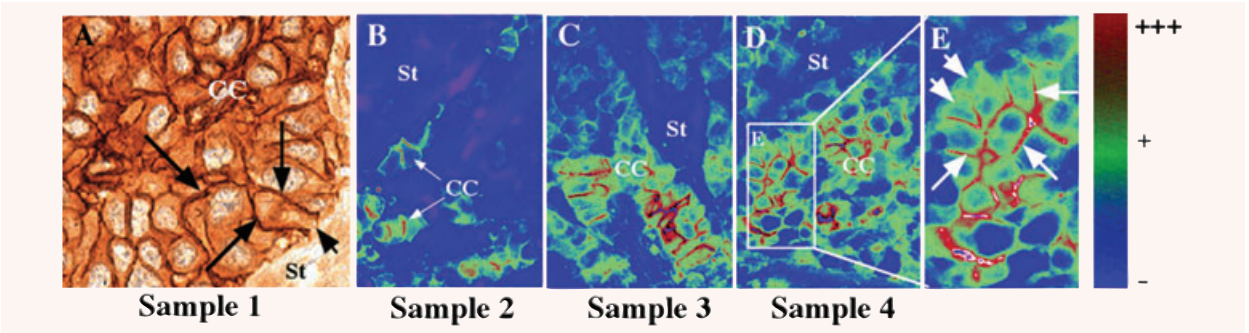

Fig. 3 Preferential localization of GLUT1 to cellular membranes involved in cell-to-cell contact. (**A**) Immunodetection of GLUT1 using peroxidase-based immunohistochemistry. The highest intensity of GLUT1 immunostaining was observed in areas of cellular membranes involved in cell-to-cell contact (arrows). (**B–E**) Semi-quantitative analysis of the preferential cellular localization of GLUT1 analysed using immunofluorescence coupled to digital image analysis in 3 different samples of grade SBRII breast cancer. The highest intensity of immunostaining was observed in cellular membranes involved in cell-to-cell contact (B–C, E – arrows). However, low level of immunostaining was observed in portions of the cellular membrane that contacted stroma (B–D, E – arrow heads). CC, cancer cells; St, stroma. Images **A**, **E**: ×600. Images **C–D**: ×300.

preferentially to the areas of the cellular membrane that seemed to be involved in cell-to-cell contact (Fig. 3A, arrows). In contrast, GLUT1 immunostaining was observed at lower intensity at portions of the cellular membrane in contact with the surrounding stroma (Fig. 3A, arrow head). Immunofluorescence coupled to digital image analyses were utilized to obtain a semi-quantitative appreciation of the level of intensity of GLUT1 immunostaining at the tissue and cellular level in three different patients (Fig. 3B–E). These studies confirmed heterogeneous expression of GLUT1 within the breast cancer parenchyma (Fig. 3B–E), with the highest levels of expression of GLUT1 localized to the areas of the cellular membranes involved in cell-to-cell contact (Fig. 3D and E, arrows). In contrast, levels of expression of GLUT1 were low-to-negative in the areas of the cellular membranes that contacted surrounding stroma (Fig. 3D and E, arrow heads).

Even though there seems to be a preferential localization of GLUT1 to the portion of the cellular membrane involved in cell-to-cell contact in SBRII breast cancer, spaces were detected between these membranes. This suggests the presence of cavities between cancer cells at these specific areas (Fig. 3C–E). Based upon this observation, immunocytochemistry coupled to transmission electron microscopy (TEM) was utilized to characterize further the putative biological role of GLUT1 at the sites of preferential localization. TEM studies were performed using 60 nm tissue sections of histological grade SBRII breast cancers (Fig. 4). Ultrastructural analyses confirmed the results obtained from standard immunohistochemistry and immunofluorescence analyses. GLUT1 localized to areas of the cellular membranes that faced neighbouring cells (Fig. 4A–C, black arrow), and GLUT1 expression was decreased in apical areas of cellular membranes exposed to the surrounding stroma (Fig. 4A–D, arrow). In the ultrastructural analyses, GLUT1 immunostaining localized mostly at cellular membranes that formed 'canaliculi-like structures' (Fig. 4A, asterisks, B, C, arrows). However, GLUT1 immunostaining was not detected in areas of cellular membranes that faced neighbouring cells but did not form the canaliculi-like structures (Fig. 4B, arrow heads).

The MDA-MB-468 cell line grown as xenografts in nude athymic BALB/c male mice mimic the preferential localization of GLUT1 observed in histological grade SBRII breast cancer

GLUT1 subcellular distribution was analysed *in vitro* using immunocytochemistry in the normal epithelial breast cell line, HMEC, and in two-breast cancer cell lines, the hormone-sensitive MCF-7, and the hormone-resistant, less differentiated and more aggressive, MDA-MB-468. In addition, subcellular localization of GLUT1 also was analysed in MDA-MB-468 grown as xenografts in nude athymic BALB/c male mice.

GLUT1 protein expression was observed in MCF-7, MDA-MB-468 and HMEC (Fig. 5). In HMEC cells, GLUT1 showed a distribution pattern that suggested intracellular localization of the protein in the perinuclear region (Fig. 5A). Low levels of GLUT1 immunostaining were detected at the cellular membrane in HMEC cells; however, GLUT1 protein was not localized to areas of the cellular membranes that faced neighbouring cells (Fig. 5C, arrow). Consistent with the *in vivo* studies, both breast cancer cell lines (MCF-7 and MDA-MB-468) showed consistently higher levels of GLUT1 immunostaining at the portion of the cellular membranes that faced neighbouring cells compared with portions of the cellular membranes that did not (Fig. 5F, I, arrows). In addition, low levels of GLUT1 immunostaining were observed with a pattern of cytoplasmic localization (Fig. 5D, F, G, I). No consistent differences in the level of expression of GLUT1 were observed between the MCF-7 and MDA-MB-468 breast cancer cell lines. Incubation of the *in vitro* specimens in the absence of the primary antibody provided the negative controls (Fig. 5B, E, H). Taken together,

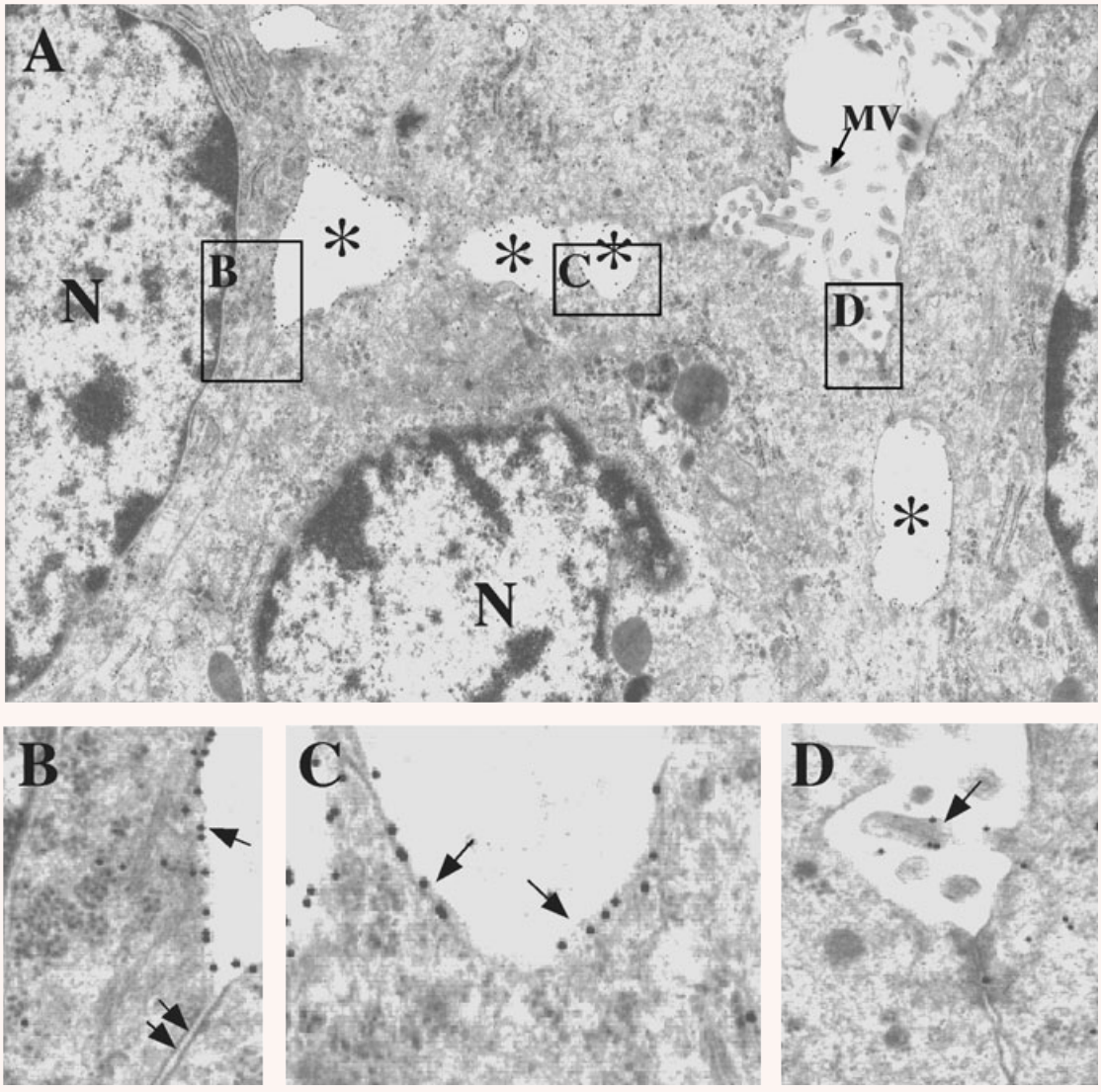

Fig. 4 Ultrastructural analysis of the GLUT1 expression in grade SBRII breast cancer. (**A**) GLUT1 subcellular localization was analysed using immunohistochemistry coupled to transmission electron microscopy (TEM). Lower panels (**B**–**D**) represent enlarged areas of the upper figure (**A**). Ultrathin sections were incubated 2 hrs with gold-labelled anti-rabbit IgG secondary antibody. Gold particles, indicative of the presence of a GLUT1 molecule, localized preferentially to areas of the cellular membranes involved in cell-to-cell contact, which associated with 'canaliculi-like structures' (**A**, **B**, **C**, asterisks and arrows). Gold particles were not observed in areas of cellular membranes involved in cell-to-cell contact, which did not form 'canaliculi-like structures' (**B**, arrow heads). Consistently lower density of gold particles was observed at the apical portion of the cellular membranes (**D**, arrow). MV: microvillus. Image **A**: ×12,000. Images **B**–**C**: 45,000.

these data confirmed the preferential subcellular localization of GLUT1 to areas of the cellular membranes that faced neighbouring cells in the breast cancer cell lines, MCF-7 and MDA-MB-468.

Expression and subcellular localization of GLUT1 in canaliculi-like structures was analysed in MDA-MB-468 cells grown as xenografts in nude athymic BALB/c male mice (Fig. 6). Histological analysis of these xenografts indicated rapid growth; cells showed a characteristic pattern of cellular columns with active proliferation (Fig. 6A, B, asterisks), and areas of cell death due to necrosis and apoptosis (Fig. 6A, arrows), that was detected using TUNEL technique (Fig. 6B, arrow). GLUT1 expression was heterogeneous within the xenograft tissue (Fig. 6C) and was associated with areas of active proliferation and increased cellular density (Fig. 6C, arrows). At the cellular level, GLUT1 localized

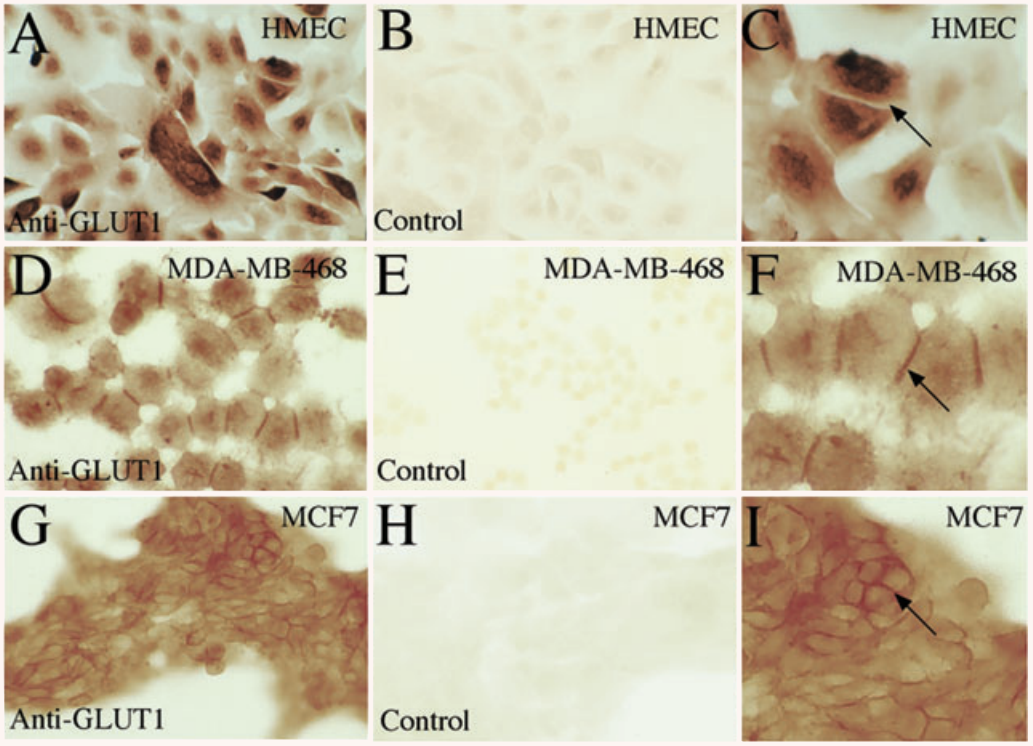

Fig. 5 Immunodetection of GLUT1 in benign and breast cancer cell lines. (**A**) Immunodetection of GLUT1 in the benign breast cell line, HMEC. (**C**) Higher magnification showed no preferential localization of GLUT1 in the HMEC cell line. (**D**, **G**) Immunodetection of GLUT1 in the breast cancer cell lines, MCF-7 and MDA-MB-468, respectively. (**F**, **I**) Higher magnification revealed preferential localization of GLUT1 to areas of the cellular membrane involved in cell-to-cell contact (F, I, arrows). (**B**, **E**, **H**) Absence of primary antibody provided negative controls. Images **A**, **B**, **D**, **E**, **G**, **H**: ×150. Images **C**, **F**, **I**: ×300.

preferentially to the cellular membranes of the cancer cells (Fig. 6C, arrows). Optic analysis of 1.0 μm thick tissue sections stained with Toluidine blue showed cancer cells organized in a columnar pattern and forming canaliculi-like structures between them (Fig. 6D, arrows). Ultrastructural analysis indicated that these tumours formed intercellular canaliculi-like structures that were limited by cellular junctions (Fig. 6E, arrows). Ultrastructural immunocytochemistry analysis demonstrated that GLUT1 localized predominantly to the cellular membrane prolongations present in these canaliculi-like structures (Fig. 6F and inset).

Discussion

Activation of GLUT gene expression for enhanced uptake and metabolism of glucose is a molecular feature of the malignant phenotype in a variety of cancers, which include breast cancer [2–7, 9, 10, 21, 23, 24, 26]. The apparent overexpression of GLUTs, especially GLUT1, suggests an important role for this transporter in cancer biology. Our group had demonstrated previously that although the isoforms GLUT2 and GLUT5 are overexpressed in human breast cancer, GLUT1 is the most widely expressed GLUT isoform. More than 90% of the human breast cancer samples expressed moderate to high levels of GLUT1 [5]. However, until now there have been no studies explaining the variability in GLUT1 expression observed among breast cancer samples. This report explores the relationship between GLUT1 expression and malignant potential in human breast cancer and provides an in depth characterization of the *in vivo* and *in vitro* subcellular localization of GLUT1 in human breast cancer cells.

The relationship between GLUT1 expression and malignant potential of human breast cancer was assessed by analysing GLUT1 mRNA and protein expression in cancers with differing histological grade, based on the Scarff-Bloom-Richardson (SBRI, II, III) grading system [30, 31]. In accordance with previous studies [7, 10], GLUT1 mRNA was overexpressed in malignant breast tissue regardless of tumour grade, compared with benign breast tissue. However, at the protein level, expression of GLUT1 was higher in samples of histological grade SBRII breast cancers compared with either SBRI or SBRIII breast cancers. Moreover, the level of GLUT1 expression associated with expression of the proliferation marker PCNA in tumours of histological grade SBRII.

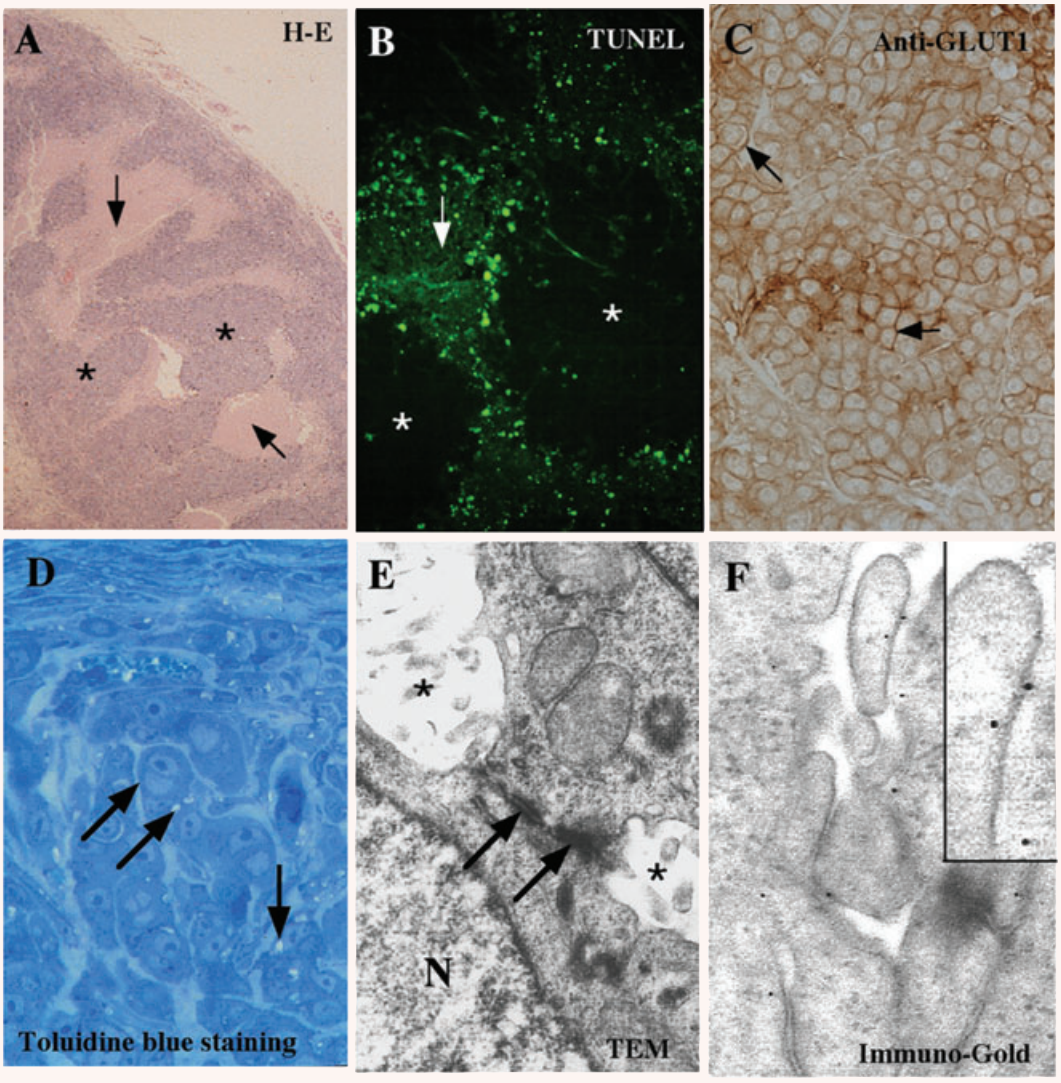

Fig. 6 Immunodetection of GLUT1 in MDA-MB-468-derived xenograft tumours induced in nude athymic BALB/c male mice. (**A**) Routine Mayer's haematoxylin and eosin stain (H&E). Histological analysis indicated a characteristic pattern of cellular columns with active proliferation (asterisk), and areas of cell death due to apoptosis or necrosis (black arrows). (**B**) Detection of cell death using the TUNEL technique in MDA-MB-468-derived xenograft tumours (white arrow). (**C**) GLUT1 immunostaining in MDA-MB-468-derived xenograft tumours. At the cellular level, GLUT1 localized preferentially to the cellular membranes of cancer cells (arrows). (**D**) Toluidine blue stain showing 'canaliculi-like structures' (arrows). (**E**) Ultrastructural analysis (TEM) of the MDA-MB-468-derived xenograft tumours showing 'canaliculi-like structures' (*) limited by cellular junctions (arrows). (**F**) Ultrastructural immunohistochemistry (immuno-gold) demonstrated GLUT1 expression at the 'canaliculi-like structures' in MDA-MB-468-derived xenograft tumours. Images **A**–**C**: ×250; **D**: ×250; **E**: ×600; **F**: ×6000; **G**: ×16,000; **H**: ×45,000. N: nucleus.

The appearance of GLUT1-positive clones in non-small cell lung carcinoma (NSCLC) has been associated with a more aggressive biological behaviour in these tumours [21]. GLUT1 expression in the colorectal carcinomas at stage T1 and T2 has been correlated to depth of invasion and histological differentiation. Furthermore, GLUT1 expression was observed to be a late event during progression of Barrett's metaplasia (BM) to carcinoma [25]. In breast cancer, Younes *et al.* [10] found GLUT1 expression in only a subset (42%) of 118 breast carcinoma tumour samples. Younes reported a weak correlation of GLUT1 expression with total histologic score, nuclear grade and percentage of cells positive for Ki-67; however, GLUT1 expression did not correlate with tumour size or lymph node metastasis.

Our findings indicated no association between GLUT1 overexpression and SBR histological grade in human breast cancer. Moreover, overexpression of GLUT1 was associated with the expression of the proliferation marker PCNA only in tumours of histological grade SBRII. One possible explanation for these inconsistent observations is that GLUT1 overexpression in breast cancer is associated with a subset of samples representative of a particularly highly proliferative tumour type. In support of this hypothesis, a positive correlation between GLUT1 expression and the proliferation marker Ki-67 has been observed in breast cancer [10], and other tumour models [22, 32, 33]. An alternative explanation for these results could be the SBR grading system. Because histological grading for breast cancer was reported first in 1925 [34], several different prognostic classifications have been introduced. The SBR grade evaluates ducto-glandular formation and nuclear pleomorphism, and currently is the most frequently used grading scheme [35]. However, SBR grading has been criticized because of its lack of reproducibility [36], a disproportionally large group of patients are placed in grade SBRII, and SBRII and SBRIII are difficult to distinguish, particularly in the subgroup of patients that are node negative [35, 37, 38]. The significance of GLUT1 as a marker of tumour differentiation as evaluated by SBR grade is unclear, and further studies will be necessary to determine whether GLUT1 overexpression can be used to subset SBR grade patients.

The relationship between GLUT1 expression and proliferation in SBRII breast cancers was explored at the cellular level by colocalization analysis of GLUT1 and PCNA using confocal laser scanning microscopy. The relationship between GLUT1 and PCNA expression was found variable; although some cells that expressed GLUT1 also expressed PCNA, some did not. Previous studies analysing the correlation between GLUT1 expression and proliferation at the cellular level are lacking; however, at the tissue level, results are controversial. A positive correlation between GLUT1 and Ki-67 expression in breast cancer specimens was documented by Younes *et al.* [10]. Another group reported contradictory results in the same tumour model [39]. In addition, no correlation was found between GLUT1 expression and cellular proliferation in colorectal adenocarcinoma cell lines [40]. Although the number of samples in our study is insufficient to establish a proper statistical correlation, our experimental observations support Younes *et al.* findings of an association between GLUT1 expression and proliferation only in grade SBRII cancers. Therefore, the characteristic expression of GLUT1 in a subset of breast tumours could explain, at least in part, divergent results found in the correlation between GLUT1 expression and proliferation. Further studies will be necessary to clarify the relationship between GLUT1 expression and proliferation at the cellular level.

The subcellular distribution of the GLUT1 in SBRII grade breast cancers was analysed using immunohistochemistry at the cellular and subcellular level. Preferential localization of GLUT1 to the areas of the cellular membrane that faced neighbouring cells was observed only in SBRII grade cancers using conventional immunocytochemistry. Ultrastructural immunohistochemistry confirmed the distribution of GLUT1 was limited to the portions of cellular membranes forming canaliculi-like structures limited by cellular junctions. A comparable pattern of expression of GLUT1 also was observed *in vitro* in the MCF-7 and MDA-MB-468 breast cancer cell lines, and in the MDA-MB-468 cell line grown as a xenograft in immunocompromised host mice. Preferential distribution of GLUT1 to canaliculi-like structures suggests a differential sorting of GLUT1 in breast cancer cells. Preferential localization of GLUT1 has been observed in highly polarized cellular models, such as human brain endothelial cells that form the blood-brain barrier [41]. In brain endothelial cells, ultrastructural analysis demonstrated a preferential localization of GLUT1 to luminal membranes, which suggests regulation of the translocation of GLUT1 from cytoplasm to the luminal membrane could explain the vectorial transport of glucose from blood to brain [41, 42]. In contrast, GLUT1 showed no preferential distribution in non-polarized cellular models, such as erythrocytes or astrocytes [43].

Verhey *et al.* [44] focused on analysis of the differential trafficking and subcellular localization of the GLUT1 and GLUT4 isoforms using recombinant chimeric transporters in which reciprocal domains were exchanged between GLUT1 and GLUT4. The carboxy-terminal 30 amino acids was responsible for differential cellular targeting of the GLUT isoforms GLUT1 and GLUT4, which suggests a putative protein domain could modulate trafficking and subcellular distribution [44]. Similar results were obtained by Mitsumoto and Klip [45] in L6 muscle cells, which indicate that subcellular distribution of GLUTs is regulated during myogenesis. Even though it is accepted that subcellular distribution of GLUTs is highly regulated in normal tissues [41, 42, 44, 45], little is known about the mechanisms that explain this regulation. Moreover, until this report, no studies have focused on the subcellular distribution of GLUTs in the cancer cell model. Our results indicate a preferential localization of GLUT1 to membrane areas involved in canaliculi-like structures in a subset of breast cancer, but not in normal epithelium, suggesting that trafficking and distribution of GLUT1 is differentially regulated in breast cancer compared with normal epithelium.

It is well established that breast cancer cells form intercellular spaces known as intercellular lumina *in vivo* and *in vitro* [46, 47]. These structures are described as abnormal secretory spaces present in between and within the breast cancer cells. However, previous ultrastructural studies of the intercellular lumina in breast cancer revealed several characteristics of these structures that are not present in the canaliculi-like structures we described: (1) Intercellular lumina usually accumulates fluid and cellular detritus within, which is observed as moderate electron-dense secretory material at the ultrastructural level, (2) Intercellular lumina are always layered by microvilli, (3) The presence of intercellular lumina is also associated with presence of intracytoplasmic lumina, which tends to displace the nucleus to one side of the tumour cells. The lack of these important features leads us to hypothesize that these canaliculi-like structures do not correspond to intercellular lumina and could therefore represent a physiological adaptation of a subset of

breast cancer cells. Even thought at this moment we do not have the proper experimental approaches to determine if these structures really correspond or not to intercellular lumina, our study suggests a putative function to these structures that has been not previously considered. Based on these observations, we hypothesize that these canaliculi-like structures or intercellular lumina could have a potential role as 'nutritional channels'. These nutritional channels may represent morpho-functional adaptations of breast cancer cells to facilitate nutrient supply, in general, and increase glucose uptake, specifically, to complement tumour neo-vascularization. Therefore, understanding the molecular mechanisms of this unusual cellular characteristic could provide a potential target to counteract increased glucose uptake in breast cancer cells.

Abbreviations

BSA, bovine serum albumin; FBS, foetal bovine serum; GLUT, glucose transporter; HRP, horseradish peroxidase; PBS, phosphate-buffered saline; SBR, Scarff-Bloom-Richardson.

Acknowledgements

The authors thank Dr. James L. Mohler from Roswell Park Cancer Institute, Buffalo, NY for the critical review of the manuscript and Dr. Carolina Delgado for assistance with pathological material. This work is supported by grant ACT-02 Conicyt-World Bank.

References

1. **Jemal A, Siegel R, Ward E, *et al.*** Cancer statistics, 2008. *CA Cancer J Clin.* 2008; 58: 71–96.
2. **Birnbaum MJ, Haspel HC, Rosen OM.** Transformation of rat fibroblasts by FSV rapidly increases glucose transporter gene transcription. *Science.* 1987; 235: 1495–8.
3. **Flier JS, Mueckler MM, Usher P, *et al.*** Elevated levels of glucose transport and transporter messenger RNA are induced by ras or src oncogenes. *Science.* 1987; 235: 1492–5.
4. **Warburg O.** On the origin of cancer cells. *Science.* 1956; 123: 309–14.
5. **Godoy A, Ulloa V, Rodriguez F, *et al.*** Differential subcellular distribution of glucose transporters GLUT1–6 and GLUT9 in human cancer: ultrastructural localization of GLUT1 and GLUT5 in breast tumor tissues. *J Cell Physiol.* 2006; 207: 614–27.
6. **Yamamoto T, Seino Y, Fukumoto H, *et al.*** Over-expression of facilitative glucose transporter genes in human cancer. *Biochem Biophys Res Commun.* 1990; 170: 223–30.
7. **Brown RS, Wahl RL.** Overexpression of Glut-1 glucose transporter in human breast cancer. An immunohistochemical study. *Cancer.* 1993; 72: 2979–85.
8. **Gould GW, Holman GD.** The glucose transporter family: structure, function and tissue-specific expression. *Biochem J.* 1993; 295: 329–41.
9. **Younes M, Lechago LV, Somoano JR, *et al.*** Wide expression of the human erythrocyte glucose transporter Glut1 in human cancers. *Cancer Res.* 1996; 56: 1164–7.
10. **Younes M, Brown RW, Mody DR, *et al.*** GLUT1 expression in human breast carcinoma: correlation with known prognostic markers. *Anticancer Res.* 1995; 15: 2895–8.
11. **Zamora-Leon SP, Golde DW, Concha II, *et al.*** Expression of the fructose transporter GLUT5 in human breast cancer. *Proc Natl Acad Sci USA.* 1996; 93: 1847–52.
12. **Tse NY, Hoh CK, Hawkins RA, *et al.*** The application of positron emission tomographic imaging with fluorodeoxyglucose to the evaluation of breast disease. *Ann Surg.* 1992; 216: 27–34.
13. **Minn H, Soini I.** [18F]fluorodeoxyglucose scintigraphy in diagnosis and follow up of treatment in advanced breast cancer. *Eur J Nucl Med.* 1989; 15: 61–6.
14. **Nieweg OE, Kim EE, Wong WH, *et al.*** Positron emission tomography with fluorine-18-deoxyglucose in the detection and staging of breast cancer. *Cancer.* 1993; 71: 3920–5.
15. **Wahl RL, Zasadny K, Helvie M, *et al.*** Metabolic monitoring of breast cancer chemohormonotherapy using positron emission tomography: initial evaluation. *J Clin Oncol.* 1993; 11: 2101–11.
16. **Levi J, Cheng Z, Gheysens O, *et al.*** Fluorescent fructose derivatives for imaging breast cancer cells. *Bioconjug Chem.* 2007; 18: 628–34.
17. **Kang SS, Chun YK, Hur MH, *et al.*** Clinical significance of glucose transporter 1 (GLUT1) expression in human breast carcinoma. *Jpn J Cancer Res.* 2002; 93: 1123–8.
18. **Laudanski P, Swiatecka J, Kovalchuk O, *et al.*** Expression of GLUT1 gene in breast cancer cell lines MCF-7 and MDA-MB-231. *Ginekol Pol.* 2003; 74: 782–5.
19. **Berlangieri SU, Scott AM.** Metabolic staging of lung cancer. *N Engl J Med.* 2000; 343: 290–2.
20. **Khandani AH, Whitney KD, Keller SM, *et al.*** Sensitivity of FDG PET, GLUT1 expression and proliferative index in bronchioloalveolar lung cancer. *Nucl Med Commun.* 2007; 28: 173–7.
21. **Younes M, Brown RW, Stephenson M, *et al.*** Overexpression of Glut1 and Glut3 in stage I nonsmall cell lung carcinoma is associated with poor survival. *Cancer.* 1997; 80: 1046–51.
22. **Hernandez F, Navarro M, Encinas JL, *et al.*** The role of GLUT1 immunostaining in the diagnosis and classification of liver vascular tumors in children. *J Pediatr Surg.* 2005; 40: 801–4.
23. **Haber RS, Rathan A, Weiser KR, *et al.*** GLUT1 glucose transporter expression in colorectal carcinoma: a marker for poor prognosis. *Cancer.* 1998; 83: 34–40.
24. **Younes M, Lechago LV, Lechago J.** Overexpression of the human erythrocyte glucose transporter occurs as a late event in human colorectal carcinogenesis and is associated with an increased incidence of lymph node metastases. *Clin Cancer Res.* 1996; 2: 1151–4.
25. **Younes M, Ertan A, Lechago LV, *et al.*** Human erythrocyte glucose transporter (Glut1) is immunohistochemically detected as a late event during malignant progression in Barrett's metaplasia. *Cancer Epidemiol Biomarkers Prev.* 1997; 6: 303–5.
26. **Garcia MA, Carrasco M, Godoy A, *et al.*** Elevated expression of glucose transporter-1 in hypothalamic ependymal cells not involved in the formation of the

brain-cerebrospinal fluid barrier. *J Cell Biochem.* 2001; 80: 491–503.
27. **Godoy A, Ormazabal V, Moraga-Cid G, *et al*.** Mechanistic insights and functional determinants of the transport cycle of the ascorbic acid transporter SVCT2. Activation by sodium and absolute dependence on bivalent cations. *J Biol Chem.* 2007; 282: 615–24.
28. **Godoy A, Watts A, Sotomayor P, *et al*.** Androgen receptor is causally involved in the homeostasis of the human prostate endothelial cell. *Endocrinology.* 2008; 149: 2959–69.
29. **Nualart F, Godoy A, Reinicke K.** Expression of the hexose transporters GLUT1 and GLUT2 during the early development of the human brain. *Brain Res.* 1999; 824: 97–104.
30. **Bloom HJ.** The value of histology in the prognosis and classification of breast cancer. *Proc R Soc Med.* 1958; 51: 122–6.
31. **Scarff RW.** Carcinoma of the breast. *Arch Middx Hosp.* 1952; 2: 174–83.
32. **Furudoi A, Tanaka S, Haruma K, *et al*.** Clinical significance of human erythrocyte glucose transporter 1 expression at the deepest invasive site of advanced colorectal carcinoma. *Oncology.* 2001; 60: 162–9.
33. **Zhou YL, Deng CS.** Correlations of expressions of Glut1 and HIF-1alpha to cellular proliferation of colorectal adenocarcinoma. *Ai Zheng.* 2005; 24: 685–9.
34. **Elston CW.** The assessment of histological differentiation in breast cancer. *Aust N Z J Surg.* 1984; 54: 11–5.
35. **Bloom HJ, Richardson WW.** Histological grading and prognosis in breast cancer; a study of 1409 cases of which 359 have been followed for 15 years. *Br J Cancer.* 1957; 11: 359–77.
36. **Le Doussal V, Tubiana-Hulin M, Friedman S, *et al*.** Prognostic value of histologic grade nuclear components of Scarff-Bloom-Richardson (SBR). An improved score modification based on a multivariate analysis of 1262 invasive ductal breast carcinomas. *Cancer.* 1989; 64: 1914–21.
37. **Davis BW, Gelber RD, Goldhirsch A, *et al*.** Prognostic significance of tumor grade in clinical trials of adjuvant therapy for breast cancer with axillary lymph node metastasis. *Cancer.* 1986; 58: 2662–70.
38. **Rank F, Dombernowsky P, Jespersen NC, *et al*.** Histologic malignancy grading of invasive ductal breast carcinoma. A regression analysis of prognostic factors in low-risk carcinomas from a multicenter trial. *Cancer.* 1987; 60: 1299–305.
39. **Haberkorn U, Ziegler SI, Oberdorfer F, *et al*.** FDG uptake, tumor proliferation and expression of glycolysis associated genes in animal tumor models. *Nucl Med Biol.* 1994; 21: 827–34.
40. **Hauptmann S, Grunewald V, Molls D, *et al*.** Glucose transporter GLUT1 in colorectal adenocarcinoma cell lines is inversely correlated with tumour cell proliferation. *Anticancer Res.* 2005; 25: 3431–6.
41. **Cornford EM, Hyman S, Swartz BE.** The human brain GLUT1 glucose transporter: ultrastructural localization to the blood-brain barrier endothelia. *J Cereb Blood Flow Metab.* 1994; 14: 106–12.
42. **Cornford EM, Hyman S, Landaw EM.** Developmental modulation of blood-brain-barrier glucose transport in the rabbit. *Brain Res.* 1994; 663: 7–18.
43. **Morgello S, Uson RR, Schwartz EJ, *et al*.** The human blood-brain barrier glucose transporter (GLUT1) is a glucose transporter of gray matter astrocytes. *Glia.* 1995; 14: 43–54.
44. **Verhey KJ, Hausdorff SF, Birnbaum MJ.** Identification of the carboxy terminus as important for the isoform-specific subcellular targeting of glucose transporter proteins. *J Cell Biol.* 1993; 123: 137–47.
45. **Mitsumoto Y, Klip A.** Development regulation of the subcellular distribution and glycosylation of GLUT1 and GLUT4 glucose transporters during myogenesis of L6 muscle cells. *J Biol Chem.* 1992; 267: 4957–62.
46. **Akhtar M, Robinson C, Ali MA, *et al*.** Secretory carcinoma of the breast in adults. Light and electron microscopic study of three cases with review of the literature. *Cancer.* 1983; 51: 2245–54.
47. **Russo J, Bradley RH, McGrath C, *et al*.** Scanning and transmission electron microscopy study of a human breast carcinoma cell line (MCF-7) cultured in collagen-coated cellulose sponge. *Cancer Res.* 1977; 37: 2004–14.